ANALYSIS OF THE STRUCTURE OF SOLUTIONS OF CHITOSAN WITH CONTROLLED DEGREES OF ACETYLATION AND POLYMERIZATION

Simina Popa-Nita[*1], Laurent David[1], Cyrille Rochas[2] and Alain Domard[1]*

[1] Laboratoire des Matériaux Polymères et des Biomatériaux – UMR CNRS 5627, Université Claude Bernard, 15 Bd A. Latarjet, Bât. ISTIL, 69622 Villeurbanne, France;

[2] Laboratoire de Spectrométrie Physique- UMR CNRS 5588, Université Joseph Fourier, 140 Av. de la Physique, B.P. 87, 38402 Saint Martin d'Hères Cédex, France

Abstract

The existence of different characteristic sizes in chitosan aqueous solutions was evidenced. At the nanoscale, Small Angle Synchrotron X-Ray Scattering revealed a polyelectrolyte correlation peak. The maximum of the polyelectrolyte peak position is given by $q_{\max} \approx \frac{2\pi}{\xi}$ where ξ scales with the polymer concentration c_p as $\xi \propto c_p^{\alpha}$; the power law exponent was found to change from $\alpha = -\frac{1}{2}$ for DA=1.5% to $\alpha = -\frac{1}{3}$ for DA=69% thus showing a structural transition from a regime where the necklace-string organization is controlled by the strings to a regime where the hydrophobic pearls are dominant in the autocorrelation of electron density. We demonstrated that the nature of the counter-ion influences the hydrophobicity of the polymer chains; chitosan hydrochloride form is found to be more hydrophobic than chitosan ethanoate or butyrate forms. At a larger scale, Static and Quasielastic Light Scattering measurements reveal the existence of 3 different size distributions: the first one is related to individual polymer coils, the second is due to the formation of nanoparticles (which is not observed for low DAs) and the last one is associated to the presence of aggregates. This organization is strictly linked to the DA confirming the existence of three domains expected by the universal law of behavior of chitosan in aqueous solutions.

Introduction

Although a wide variety of chitosan macroscopic properties are already used for industrial applications (agro-food domain, cosmetics, water treatment), the organization of such materials and solutions at the micro and nanoscopic ranges are not completely understood. The difficulty of explaining chitosan behavior in aqueous solutions comes from its character of polyelectrolyte exhibiting both cationic and hydrophobic sites along its chain. Thus, chitosan physical, chemical and biological properties and its conformation in aqueous solutions depend on various structural parameters (degree of acetylation, degree of polymerization, distribution of the residues along the chain) but also on external parameters (pH, ionic strength, dielectric constant of the solvent, etc.). Our aim was to gain insight into the molecular organization of chitosan by analyzing the heterogeneity of its aqueous solutions at various scales.

Materials and Methods

Purification and acetylation of chitosan

The initial chitosan produced from squid pens was procured from Mahtani Chitosan Limited. The polymer was subject to a first step of purification, which consisted in dissolving chitosan at 0.5%

(w/v) in a stoechiometric amount of aqueous acetic acid. The solution obtained was filtered successively on 3, 1.2, 0.8 and 0.45 µm membranes and then the polymer was precipitated using aqueous ammonia. After repeated washings with deionized water, the precipitated polymer was finally freeze-dried.

Chitosans of different DAs were prepared from the reacetylation under soft conditions of a highly deacetylated chitosan (DA=1.5%) in a fresh solution of acetic anhydride and propanediol thus allowing the preservation of a statistical distribution of residues within the chains*[1]*. The reacetylation reaction was followed by precipitation adding aqueous ammonia and by repeated washings with deionized water. Reacetylated chitosans at the highest DAs were fully soluble in water whatever the pH and so an organic solvent was used to precipitate and wash the samples. In this case, acetic acid and acetate salt were removed by dialysis.

A first characterization of the obtained samples was performed by ^{1}H NMR Spectroscopy (to verify the DA) *[2]* and by Size Exclusion Chromatography coupled with a differential refractometer and a multiangle laser-light scattering detector (to determine the molecular weight and the gyration radius). The results are given in Table 1.

DA (%)	M_w (10^5 g/mol)	Ip	$R_{G,z}$ (nm)
1.5 ± 0.1	5.102 ± 0.047	1.6 ± 0.1	129 ± 9
9.0 ± 0.1	5.539 ± 0.065	1.6 ± 0.1	131 ± 4
14.5 ± 1.0	5.945 ± 0.078	1.7 ± 0.2	141 ± 7
24.2 ± 1.0	5.641 ± 0.059	1.7 ± 0.1	124 ± 6
38.0 ± 0.5	6.226 ± 0.094	1.7 ± 0.1	135 ± 7
41.1 ± 0.1	6.146 ± 0.085	1.7 ± 0.2	138 ± 9
51.2 ± 0.1	3.355 ± 0.072	1.7 ± 0.2	84 ± 6
68.7 ± 0.5	4.485 ± 0.061	1.7 ± 0.1	91 ± 5

Table 1: Characteristics of reacetylated chitosans

Preparation of solutions

Chitosan was dispersed in acetic, butyric or hydrochloric aqueous solutions with stoechiometric protonation of $-NH_2$ sites.

For the quasielastic light scattering measurements, salt had to be present in the polyelectrolyte solutions to minimize the electrostatic contributions by screening ionic sites along the chains. Thus chitosan was dispersed in an acetic acid/ammonium acetate buffer *[3]*.

Both types of solutions were stirred overnight to allow complete dissolution of the polymer.

Small Angle Synchrotron X-Ray Scattering

SAXS measurements were performed at the ESRF (European Synchrotron Radiation Facility) on the BM2-D2AM beamline. The primary data corrections (dark current, flat field response and tapper distortion) were carried out using the software available on the beamline. Silver behenate was used as a *q*-range calibration. As an additional correction, the contribution of the cells filled with water was subtracted to scattering response of the samples.

Quasielastic Light Scattering (QELS)

QELS measurements were performed with an argon laser working at a wavelength of 448nm and equipped with a goniometer and a correlator ALV-5000. Experiments were done at a fixed angle equal to 90°. The obtained intensity correlation functions of the scattered light were used to determine the size distribution of the samples (regularization method Contin *[4]*) and the polymer hydrodynamic radii (method of cumulant *[5]*).

Results and Discussion

Polyelectrolyte ordering of chitosan solutions

The interaction of hydrophobic charged polymer chains is rather complex and in order to capture a global view of it, an analysis must be performed at different length scales. At the larger scale, two

different organizations coexist: dissolved polyelectrolyte chains and chain aggregates. The description of the first one leads, at a smaller scale, to the pearl necklace model *[6]*. At low charge density, the polymer chain conformation corresponds to a succession of electrostatic blobs *[7]*. When the charge density increases, the electrostatic blob divides into smaller hydrophobic globules (the so-called "pearls") linked together by more extended segments (the so-called "strings"). Finally, at a local scale, the formation of a counter-ion layer around the polymer chain *[8]* induces the decrease of the effective charge carried out by the polymer and is also believed to induce long range effects.

From an experimental point of view, we analyzed chitosan solutions through the polyelectrolyte correlation peak appearing on the Small Angle Synchrotron X-ray Scattering Curves, following the relation:

$$I(q) = D + \frac{C}{q^{\gamma}} + \frac{B}{1 + 4\left(\frac{q - q_{\max}}{w}\right)^2},$$

where $q_{\max}$ represents the position of the maximum, w the FWHL and B the intensity of the Lorentzian peak. The second term of the formulae represents the contribution of large range electronic density fluctuations and D takes into account the incoherent scattering and amourphous halo, contributions neglected in many cases.

The scattering diagrams of chitosan solutions corresponding to three counter-ions: hydrochloride, ethanoate and butyrate are presented on Figure 1. A study was done for different polymer concentrations raging from 5 to 20g/l for a chitosan of DA equal to 1.5%.

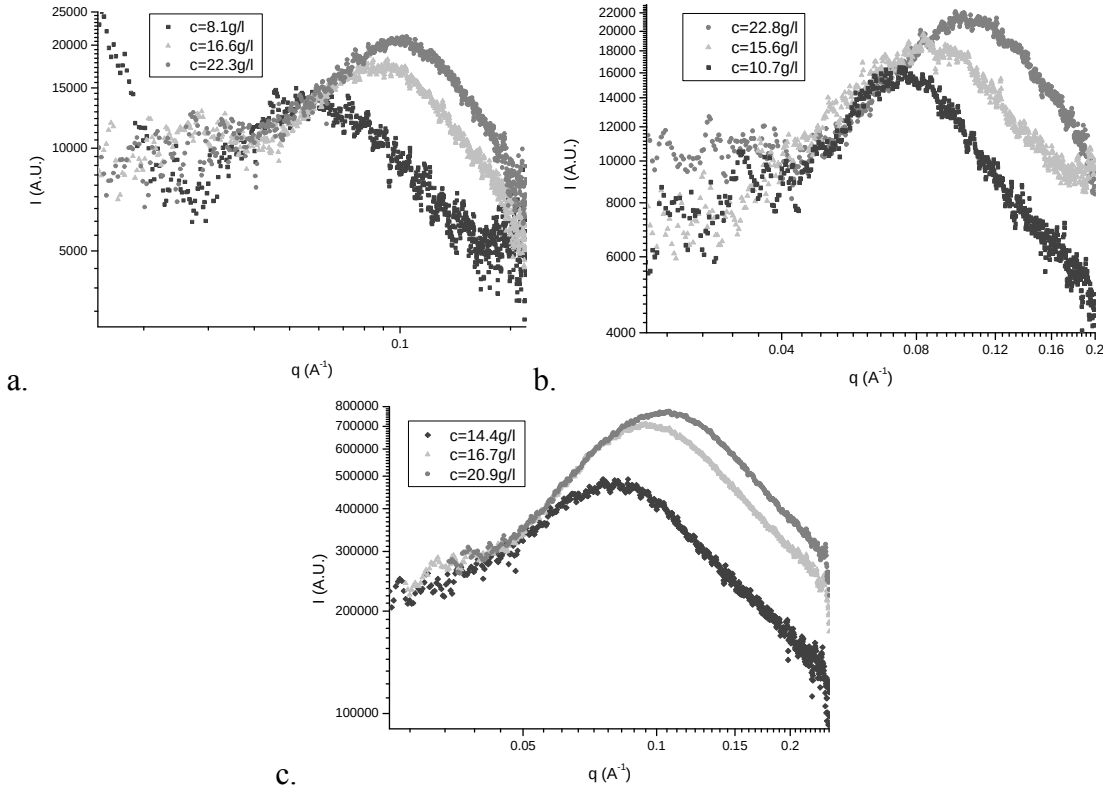

Figure 1 : SAXS diagrams of (a) hydrochloride, (b) ethanoate and (c) butyrate chitosans of DA=1.5%

For all the counter-ions studied, the amplitude and the position of the maximum of the polyelectrolyte peak increase with the polymer concentration. From the location of this peak, one can deduce the value of the interchain or correlation distance as $\xi \approx \frac{2\pi}{q_{\max}}$. The plot representing the variation of ξ as a function of the polymer concentration c_p for the same chitosan (DA=1.5%) and the three counter-ions is shown on Figure 2.

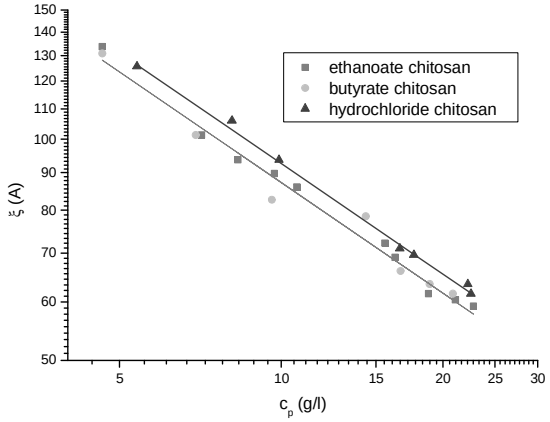

Figure 2 : Scaling relation of the interchain distance in chitosan hydrochloride, ethanoate and butyrate forms as a function of the polymer concentration. Solid lines represent the $(c_p)^{-1/2}$ law

In this case, the degree of acetylation is below the Manning condensation threshold; chitosan is a strong polyelectrolyte of high charge density dispersed in a polar solvent of good quality so that ξ varies as $c^{-1/2}$ in the whole concentration range, as expected *[9]*.

Figure 2 also shows the influence of the nature of the counter-ion: the curve corresponding to the hydrochloride form of chitosan is systematically above those related to the ethanoate and butyrate forms. No difference is noticed between these last two counter-ions. We can then deduce that the hydrochloride chitosan corresponds to a more hydrophobic polymer than chitosan ethanoate or butyrate for low DAs (high charge density)*[10]*.

Molecular association simulations showed *[11]* that ethanoate ions (and following the same argument, butyrate ions too) could interact (electrostatic and hydrogen bonding) with glucosamine residues, more precisely with the amine site and the OH group of the carbon 3 thus forming a complex. On the other hand, hydrogen bonding can not involve chloride anions and thus the ion pairs corresponding to hydrochloride chitosan do not promote its solubility in water.

At high DAs (low charge density), α, the exponent of the power law of variation of ξ with the polymer concentration becomes equal to $-\frac{1}{3}$ as it can be seen on the Figure 3.

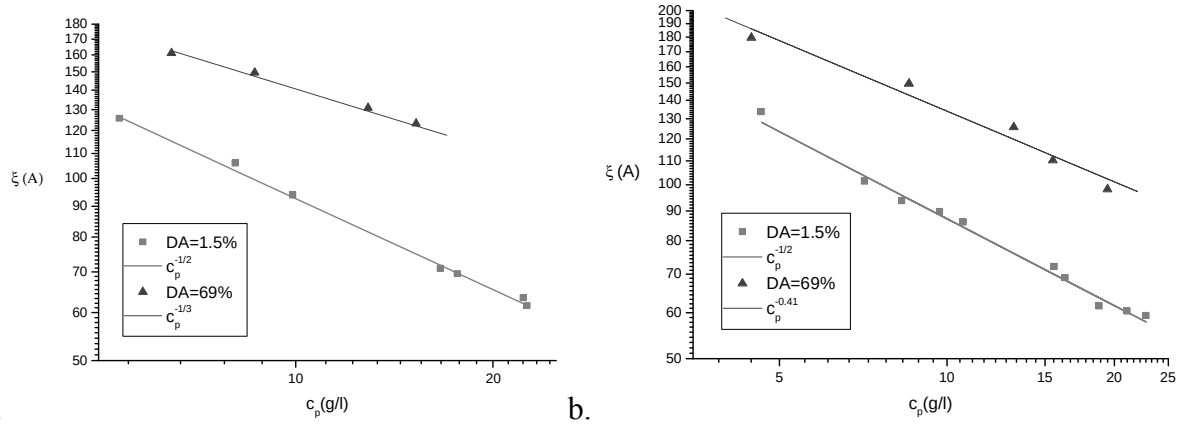

Figure 3 : Scaling relation of the interchain distance in chitosan (a) hydrochloride and (b) acetate forms as a function of the polymer concentration for DA=1.5 and 69%. Solid lines represent the $(c_p)^{-1/2}$ and $(c_p)^{-1/3}$ laws

The pearl necklace model for solvophobic polymers *[6]* explains these results in terms of a transition from a string controlled domain ($\alpha = -\frac{1}{2}$) to an organization dominated by the hydrophobic pearls ($\alpha = -\frac{1}{3}$).

Extended scattering diagram

At a larger scale of organization, chitosan solutions were analyzed by Static Light Scattering at small and wide angles. For a hydrochloride form of chitosan of DA=1.5%, the information we gathered for a size scale below the chain length (SAXS measurements) was completed by WALS results as shown on Figure 4.

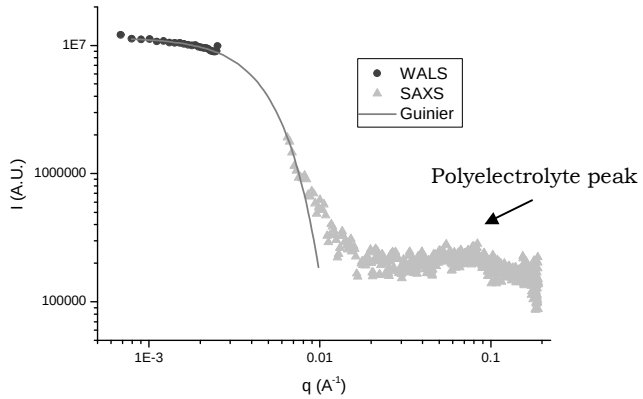

Figure 4 : WALS and SAXS diagrams for a hydrochloride chitosan of DA=1.5%, c=10g/l. Solid line represents the Guinier law

The shape of the scattering curves could be interpreted using the Guinier law: $I = I_0 \exp\left(-\frac{R_g^2}{3}q^2\right)$, where I_0 is the incident intensity and R_g the polymer gyration radius. In this case, we find a value of the gyration radius of 36nm, which is in agreement with an organization of individual polymer coils.

Furthermore, the scattering diagram of the analyzed hydrochloride chitosan can be broaden by adding SALS results, Figure 5.

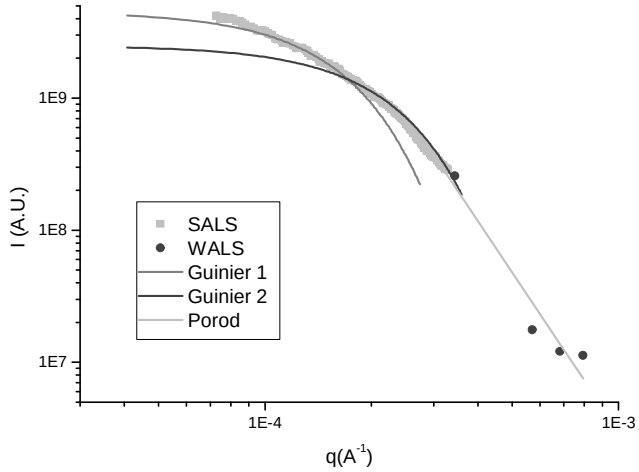

Figure 5 : SALS and WALS diagrams for a hydrochloride chitosan of DA=1.5%, c=10g/l. Solid lines represent the Guinier and Porod laws

In the SALS range, the morphology is too complex to be described by a simple Guinier law; the use of the sum of at least two Guinier contributions yielding respective gyration radii of 0.8µm and 1µm is needed. As a result, at least 3 levels of organization can be described in chitosan solutions for a DA of 1.5%: in the size range close to 1µm i.e. at the larger length scale studied here, polymer chain aggregates are observed but they coexist with individual polymer coils and the nanoscopic ordering due to polyelectrolyte chains.

Size distributions determined by QELS

These different characteristic sizes in the structural organization of chitosan solutions can be verified by analyzing the relaxation modes by QELS.

For several reasons (minimize the electrostatic contributions, decrease the viscosity), chitosan was dispersed in an acetic acid/ammonium acetate buffer.

For chitosan of DA=1.5% present in the solutions at concentrations ranging from 0.1 to 3g/l, the result given by the Contin method *[4]* is a single peaked distribution of the hydrodynamic radii. This distribution corresponds to a unique although rather broad population of polymer species, in agreement with the gyration radius calculated by WALS measurements. Furthermore, we notice a deviation of the population toward the shorter relaxation times when the concentration increases. This variation of the hydrodynamic radii (calculated by the method of cumulant *[5]*) as a function of the concentration is shown on Figure 6.

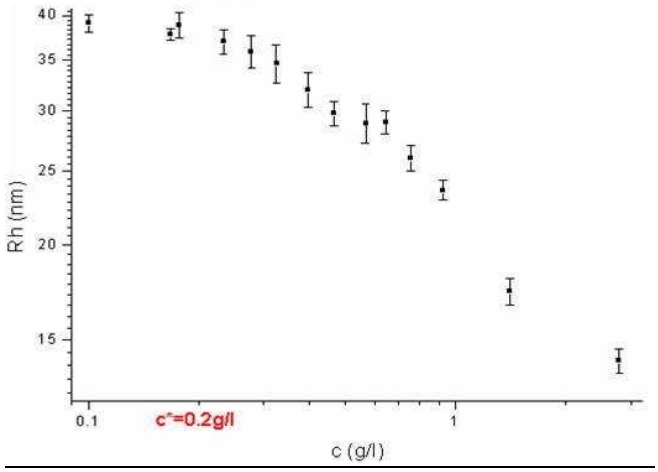

Figure 6 : Variation of the hydrodynamic radii as a function of the concentration for chitosan of DA=1.5%

Different laws of variation are noticed before and after a critical concentration of 0.2g/l. The same solutions were analyzed by Static Light Scattering and by means of Zimm plot, we could determine the weight average molecular weight (M_w) and the root-mean-square z–average of the gyration radius (R_g) for this chitosan. From these parameters, we calculated *c**, the critical concentration for chain entanglement by using the Fox Flory formulae:

$[\eta] = 6^{\frac{3}{2}} \Phi_0 \frac{< R_G^2 >^{\frac{3}{2}}}{M_w}$, where [η] is the intrinsic viscosity, $[\eta] \approx \frac{1}{c^*}$ and $\Phi_0 = 2.87 \times 10^{23} mol^{-1}$. We found that *c** is equal to 0.2g/l again.

For low DAs, i.e. for a high charge density, chitosan follows the behavior predicted by the Manning condensation; as the solution concentration increases, the ionic strength is high resulting in a decrease of the hydrodynamic radii. This argument is also verified by the R_h invariance with the solution concentration for chitosan of DA=69%. In this case, the ionic strength is indeed poorly influenced by the variation of the concentration.

Nevertheless, for high DA values, we notice the presence of a second peak corresponding to longer relaxation times. This second population has a hydrodynamic radius of about 200nm and corresponds to a few interacting polymer chains forming nanoparticles. For an intermediate value of DA (37%), we notice a broadening of the peak related to the individual polymer chains but no nanoparticle distribution is observed.

For all the analyzed chitosans, a peak related to the presence of aggregates of size exceeding 1µm is also observed. This distribution confirms the gyration radii calculated by the Guinier laws used to explain the SALS results.

These results should be related to the universal law of behavior of chitosan characteristics in aqueous solutions as a function of DA. It was demonstrated *[12]* that when DA increases, chitosan properties change through three distinct domains. Below 30%, chitosan behaves as a strong polyelectrolyte and the Manning theory of ionic condensation is verified. Above 50%, chitosan is a hydrophobic polymer with isolated charges on its chains. In-between, there is a transition range where the properties barely vary with DA.

Conclusion

This study brings new elements for the characterization of heterogeneous chitosan solutions. The organization of these systems is very complex and concerns different size scales. At a local scale, by investigating the so-called "polyelectrolyte peak", we conclude that for low DAs the structure of the necklace model is controlled by the strings between the pearls and for high DAs, the hydrophobic pearls are dominant. We also show that the nature of the counter-ion influences the environment of the polymer chains, chitosan hydrochloride being more hydrophobic than ethanoate or butyrate forms. At a larger scale of organization and when specific conditions are met (DA, DP, pH), the existence of chitosan nanoparticles is evidenced. This was revealed by QELS analysis. Finally, at the largest length scale, polymer aggregates are observed. The equilibriums between these populations (polymer chains, nanoparticles, aggregates) depend on various parameters such as: degree of acetylation, pH, ionic strength, ageing time, temperature etc. We also brought about new arguments in favor of the universal law of behavior of the physico-chemical properties of chitosan as a function of DA.

Acknowledgement

These studies are part of the NanoBioSaccharides project from the 6th European Framework Program "Nanotechnologies and nanosciences, knowledge-based multifunctional materials and new production processes and devices". We also are indebt for the assistance of Jean-Michel Lucas and Agnès Crepet.

References

[1] Sorlier P., Denuzière A., Viton C.and Domard A., Biomacromolecules 2001, 2, 765

[2] Hirai A., Odani H.and Nakajima A., Polm. Bull. 1991, 26, 87

[3] Domard A.and Rinaudo M., Polym. Commun 1984, 25, 55

[4] Provencher S. W., Makromol. Chem. 1985, 82, 632

[5] Koppel D. E., J. Chem Phys. 1972, 57, 4814

[6] Dodrynin A.V. and Rubinstein M., Macromolecules, 2001, 34, 1964

[7] De Gennes P.G., Pincus P. and Velasco R.M., Journal de Physique, 1976, 37, 1461

[8] Manning G.S., Biophysical Chemistry, 1977, 7, 95

[9] Waigh T.A., Ober R., Williams C.E. and Galin J.C., Macromolecules, 2001, 34, 1973

[10] Essafi W., Lafuma F. and Williams C.E., European Physical Journal *B*, 1999, 9, 261

[11] Terreux R., Domard M. and Domard A., Advances in Chitin Science, 2006 (this issue)

[12] Montembault A., Viton C. and Domard A., Biomacromolecules, 2005, 6, 653